

# Simultaneous Spectrophotometric Determination of Cd<sup>2+</sup>, Cu<sup>2+</sup>, and Zn<sup>2+</sup> in Rice and Vegetal Samples with Dimethyl-spiro[isobenzofurane-1,6'-pyrrolo[2,3-d]pyrimidine]-2',3,4,5'(1'H,3'H,7'H)tetraone Using Wavelet Transformation–Feed Forward Neural Networks

Maryam Abbasi Tarighat,<sup>\*,†</sup> Mohammad Reza Mohammadzadeh,<sup>†</sup> and Gholamreza Abdi<sup>‡</sup>

<sup>†</sup>Department of Chemistry, Faculty of Sciences, Persian Gulf University, Bushehr 75169, Iran

<sup>‡</sup>Department of Biotechnology, Persian Gulf Research and Studies Center, Persian Gulf University, Bushehr 75169, Iran

**ABSTRACT:** A multicomponent analysis method for the simultaneous spectrophotometric determination of the Cd<sup>2+</sup>, Cu<sup>2+</sup>, and Zn<sup>2+</sup> based on complex formation with dimethyl-spiro[isobenzofurane-1,6'-pyrrolo[2,3-d]pyrimidine]-2',3,4,5'(1'H,3'H,7'H)tetraone using wavelet transformation–feed forward neural network is proposed. The analytical data showed that metal to ligand ratios in all metal complexes was 1:1. The absorption spectra were evaluated with respect to synthetic ligand concentration and pH. It was found that, at pH 6.7, the complexation reactions were completed. Spectral data were reduced using continuous wavelet transformation (CWT) and subjected to artificial neural networks. The presence of nonlinearities was confirmed by a partial response plot. The structures of the CWT–feed forward neural networks (WT-FFNN) were simplified using the corresponding wavelet coefficients of mother wavelets. Once the optimal wavelet coefficients are selected, different ANN models can be employed for the calculation of the final calibration model. The proposed methods were successfully applied to the simultaneous determination of Cd<sup>2+</sup>, Cu<sup>2+</sup>, and Zn<sup>2+</sup> in rice, dill, tomato, and lettuce samples.

**KEYWORDS:** *isobenzofurane, simultaneous determination, Cd<sup>2+</sup>, Co<sup>2+</sup>, Zn<sup>2+</sup>, CWT, FFNNs*

## ■ INTRODUCTION

The content of trace elements in different samples is important and of great interest due to human exposure and environment parameters. Vegetable and fruit samples can contain toxic metals from their presence in the soil, water, or air. High levels of toxic metals can be found when agricultural expedients such as fertilizers and pesticides are used. People are exposed to toxic metals mainly by eating foods containing them, breathing contaminated workplace air, or drinking contaminated water.<sup>1</sup>

Trace metal ions in foods can produce undesirable effects such as discoloration, turbidity, and oxidation. The chelating agent can form a complex with the unwanted trace metals, thus blocking the reactive sites of the metal ions and rendering them inactive.<sup>2</sup>

Cadmium, and its inorganic compounds, is probably the most potentially toxic metal in the environment. It has no known nutritional or beneficial effects on human health but is ubiquitous in nature and present in air, water, fertilizer, fungicides, soil, rice, coffee, tea, and soft drinks, so that some level of exposure is not readily preventable.<sup>3</sup> Cadmium accumulates in the body and has various degrees of toxicity. It is used in the production of colored inks and dyes, as well as in many industrial applications, such as metal plating, engraving, and soldering.

Copper is relatively nontoxic. Copper deficiency reduces productions of both red and white blood cells, causing anemia and poor immune function.<sup>3</sup> However, in Wilson's disease, a rare genetic disorder, excessive copper accumulates in the liver, brain, kidney, and eye. Like copper deficiency, copper excess

causes anemia. Zinc supplements, which inhibit copper absorption, also are used in treating Wilson's disease. Because the body gets rid of excess zinc efficiently, high dietary zinc intake toxicity is rare. Yet there have been isolated accounts of acute zinc toxicity in people who consumed large amounts of acidic foods.<sup>1</sup>

Accurate determination of trace metals may help to elucidate their role and function in the different areas. Hence, there is an ongoing requirement to develop analytical methodologies for their sensitive and selective determination in many sample types. Flame atomic absorption spectrometry (FAAS),<sup>4–7</sup> inductively coupled plasma–optical emission spectrometry (ICP-OES),<sup>8</sup> spectrophotometric least-squares fit,<sup>9</sup> flow-through anodic stripping coulometry and anodic stripping coulometry,<sup>10</sup> derivative potentiometric stripping,<sup>11,12</sup> flow injection zone sampling,<sup>13</sup> solid phase extraction using magnetic nanoparticles<sup>14</sup> and chromatography,<sup>15</sup> and membrane filtration<sup>16</sup> are used for the determination of cadmium, copper, and zinc in different samples.

The necessary step before the instrumental analysis is, in many cases, the destruction of the organic matter present in the food samples, called “digestion”. This procedure is a form of oxidation caused by atmospheric oxygen in the dry ashing method or by oxidizing acids in the wet digestions; different

**Received:** March 6, 2013

**Revised:** June 9, 2013

**Accepted:** June 17, 2013

**Published:** June 17, 2013

types of wet digestions can be performed, using the assistance of various techniques.

In this continuation, Soylak et al. applied a microwave-assisted digestion procedure for the determination of zinc, copper, and nickel in different tea samples.<sup>17</sup> Also, mineral content of Turkish multifloral honeys had been determined by flame and graphite atomic absorption spectrometry techniques after dry ashing, microwave digestion, and wet digestion.<sup>18</sup>

Even sensitive and accurate determination of heavy metals has been continuously performed by FAAS, but the relatively lower element concentrations than detection limits of FAAS is one of the main difficulties in these determinations.<sup>16</sup> Interferic effects sourced from the matrix of the real sample is another problem in FAAS determinations, which make concomitant ions influence the quantitation limit.<sup>16,20,21</sup> In using the FAAS method to remove sample matrix interferences and/or preconcentration, the use of exchange sorbents is often required.<sup>19</sup> This means that, despite the significant analytical chemical capacity, FAAS often requires a suitable pretreatment step (separation) of the sample, to facilitate the desired sensitivity and selectivity of the measurement.<sup>22,23</sup> Another disadvantage of the AAS measurements is that only a single element can be determined at a time as a separate radiation source is required for each element.<sup>20</sup> However, new methods are needed to undertake multielement determinations.

Of the other methods reported in the literature on the determination of metal ions, we address the chemometrics methods. Various methods including multivariate calibration methods (partial least-squares (PLS) or principal component regression (PCR)), iterative target transformation,<sup>24,25</sup> and artificial neural networks<sup>26,27</sup> have been used for multi-component determination.

Wavelet transform is very efficient for removing baseline effect, reducing noise, and data compressing. Few papers have been published on the application of wavelet transformation (WT) for simultaneous determination of chemical species.<sup>28</sup> The combined use of continuous wavelet transformation (CWT) and zero-crossing was first formulated by Dinc and Baleanu, for the quantitative resolution of two-component mixtures.<sup>29,30</sup> Recently, we applied CWT for the determination of enantiomeric ratios.<sup>31</sup>

The accurate and precise determination of metal ions in environmental, biological, pharmaceutical, food, and water samples is the main interest area of our research. In this way, we have carried out some studies on the application of new selective ligands in the spectrophotometric determination of different species.<sup>32,33</sup> Also, we used bromopyrogallo red (BPR) at pH 9.40 for the simultaneous determination of ternary mixtures of calcium, magnesium, and zinc in different foodstuffs and pharmaceutical samples, by ratio spectra–continuous wavelet transformation.<sup>29</sup> We have further performed simultaneous determination of Co<sup>2+</sup>, Ni<sup>2+</sup>, Cu<sup>2+</sup>, and Zn<sup>2+</sup> in different vegetables, foodstuffs, and pharmaceutical product samples with a synthesized Schiff 3,6-bis((aminoethyl)thio)pyridazine.<sup>26</sup> The applicability of radial basis function networks for kinetic–spectrophotometric determination of Sn(II) and Sn(IV) in water and juices of canned fruits as evaluated.<sup>33</sup>

As the continuation of our previous work, the applicability of a new synthetic ligand derived from bis(pyrazole) was examined for the simultaneous determination of Fe<sup>3+</sup> and Mn<sup>2+</sup> in some food, vegetable, and water samples by artificial neural networks.<sup>34</sup>

Also, we applied ratio spectra–continuous wavelet transformation for the simultaneous determination of ternary mixtures of copper, cobalt, and nickel with 1-(2-pyridylazo)-2-naphthol (PAN) without prior separation steps.<sup>35</sup>

In this work we examined the applicability of a new synthetic spiro ligand for the simultaneous determination of metal ions using artificial neural networks (ANNs). Despite the good performance of ANNs, we propose a methodology, based on the wavelet transform which is multiresolution analysis, for feature selection prior to calibration.<sup>28</sup> This means that, in the present study not only the advantages of WT in extraction of characteristic information but also the advantages of ANNs in nonlinear models were applied. It is nowadays accepted that there is a benefit from data transformation aiming at removing baseline effect, reducing noise, and synthesizing and compressing the data. In the present work, we adopted a simplified approach whereby, instead of using PCA, the selection of the wavelet coefficient to be used as the predictor variables is done by the calculation of variance vector. Once the optimal wavelet coefficients are selected, different ANN modes can be employed for the calculation of the final calibration model. The selected coefficients constitute a set of independent variables, which can be fed to ANN models. Hence, the key concepts of our methodology are revealing the independent variables and reducing the number of data to accelerate the design of ANNs for accurate prediction of concentrations. The proposed methods were successfully applied to the simultaneous determination of multicomponent overlapping spectra of Cd<sup>2+</sup>, Cu<sup>2+</sup>, and Zn<sup>2+</sup> in the presence of nonlinearity. The method was validated by the simultaneous determination of desired ions in synthetic and dill, rice, tomato, and lettuce samples.

## THEORY

**Wavelet Transform.** Wavelet bases, like Fourier bases, reveal the signal regularity through the amplitude of coefficients, and their structure leads to a fast computational algorithm. However, wavelets are well localized, and few coefficients are needed to represent local transient structures. As opposed to a Fourier basis, a wavelet basis defines a sparse representation of piecewise regular signals, which may include transients and singularities.<sup>36</sup> Continuous wavelets are functions used by the continuous wavelet transform. The original signal can be reconstructed by suitable overall integration of the resulting frequency components after projection of a given signal on a continuous family of frequency bands. The subspace of scale  $a$  or frequency band is generated by the function

$$\psi_{(a,b)}(t) = \frac{1}{\sqrt{a}} \psi\left(\frac{t-b}{a}\right) \quad (1)$$

where  $a$  is positive and defines the scale and  $b$  is any real number and defines the shift. The original signal can be reconstructed by suitable integration over all of the resulting frequency components after projection of a given signal on a continuous family of frequency bands.

Selection of an appropriate wavelet filter may be guided by empirical rules applied to data size and signal continuity. The typical way is to visually inspect the data first and then select an appropriate wavelet filter.<sup>37</sup>

In addition to wavelet function, dilation (scaling factor) has also an important role to get maximum resolution and

sensitivity. A proper dilation was selected using the criterion introduced by Xiaoquan et al.<sup>38</sup>

$$\text{fitness}(a) = \sum_{b=1}^{\text{length}f(x)} [|\text{Wf}_{(a)}(b)| - |f(b)|]^2 \quad (2)$$

Fitness ( $a$ ) represents the accumulated difference between the wavelet coefficients  $\text{Wf}_{(a)}(b)$  and the original data at each transition. The dilation that makes fitness ( $a$ ) have the minimum value would be chosen as the best.

To select the wavelet coefficients, for example, for a matrix of size  $N \times K$ , the variance vector is calculated as

$$\text{variance}_k = \frac{\sum (X_{nk} - \bar{X}_k)^2}{N - 1} \quad (3)$$

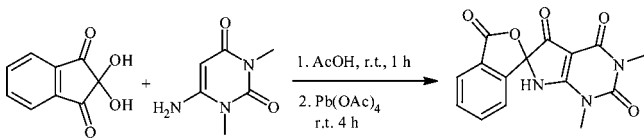
$k = 1, 2, \dots, K$  (column index), and  $n = 1, 2, \dots, N$  (row index).

## EXPERIMENTAL PROCEDURES

**Reagent and Standard Solutions.** Chemicals were purchased from Sigma-Aldrich and Merck (Darmstadt, Germany) and used as received with no further purification. Stock solutions of  $\text{Cu}^{2+}$ ,  $\text{Co}^{2+}$ , and  $\text{Zn}^{2+}$  ( $1000 \text{ mg L}^{-1}$ ) were prepared by dissolving  $\text{CuCl}_2$ ,  $\text{Cd}(\text{NO}_3)_2$ , and  $\text{ZnCl}_2$  in deionized water. A  $0.834 \text{ mmol L}^{-1}$  dimethyl-spiro[isobenzofurane-1,6'-pyrrolo[2,3-*d*]pyrimidine]-2',3,4,5'(1'*H*,3'*H*,7'*H*)tetraone (DMSPT) solution was prepared by dissolving it in 80:20 (v/v) acetonitrile/ $\text{H}_2\text{O}$ . A phosphate buffer solution of pH 6.7 ( $0.2 \text{ mol L}^{-1}$ ) obtained by mixing  $\text{KH}_2\text{PO}_4$  and  $\text{Na}_2\text{HPO}_4$  was prepared.

**Preparation of Dimethyl-spiro[isobenzofurane-1,6'-pyrrolo[2,3-*d*]pyrimidine]-2',3,4,5'(1'*H*,3'*H*,7'*H*)tetraone (Scheme 1).** A mixture of ninhydrin 3 (1 mmol) and 6-aminouracil 4

**Scheme 1. Synthesis of Dimethyl-spiro[isobenzofurane-1,6'-pyrrolo[2,3-*d*]pyrimidine]-2',3,4,5'(1'*H*,3'*H*,7'*H*)tetraone**



(1 mmol) in AcOH (3 mL) was stirred at room temperature for 1 h.  $\text{Pb}(\text{OAc})_4$  (1.1 mmol) was added and stirring continued for a further 4 h, and then  $\text{H}_2\text{O}$  (10 mL) was added. The reaction mixture was filtered and washed with hot  $\text{H}_2\text{O}$  ( $2 \times 5 \text{ mL}$ ), and the obtained product was further purified by recrystallization from EtOH (Merck).

Overall yield, 90%; mp  $>300 \text{ }^\circ\text{C}$ ; IR (KBr,  $\text{cm}^{-1}$ ), 3379, 1764, 1743, 1666, 1601, 1520;  $^1\text{H}$  NMR (500 MHz,  $\text{DMSO}-d_6$ ),  $\delta$  3.12 (s, 3H,  $\text{CH}_3$ ), 3.67 (s, 3H,  $\text{CH}_3$ ), 7.69 (dt,  $J_1 = 7.5 \text{ Hz}$ ,  $J_2 = 1 \text{ Hz}$ , 1H, arom), 7.80 (t,  $J = 7.2 \text{ Hz}$ , 2H, arom), 7.87 (dt,  $J_1 = 7.5 \text{ Hz}$ ,  $J_2 = 1 \text{ Hz}$ , 1H, arom), 8.30 (s, 1H, NH);  $^{13}\text{C}$  NMR (125 MHz,  $\text{DMSO}-d_6$ ),  $\delta$  28.4, 37.6, 94.6, 99.1, 125.4, 125, 9130.5, 132.4, 136.8, 143.2, 151.8, 157.2, 166.4, 168.1, 186.4; MS (70 eV),  $m/z$  (%) 313, ( $\text{M}^+$ , 55), 285 (100) 257 (98), 200 (84), 105 (80).

**Apparatus and Data Processing.** A model 713 Metrohm pH meter using a combined glass electrode was used for the pH measurement of solutions. A detection system consisting of an Analytical Jena SPECORD250-22P16 UV-vis double-beam spectrophotometer using 1 cm quartz cells, slit of 0.5 cm, and scan speed of  $100 \text{ nm s}^{-1}$  was selected. The recorded spectra were digitized with one data point per nanometer. The network calculations were performed using nnet-Toolbox for MATLAB 7.1.

**Procedure.** A series of mixtures as calibration, prediction, and validation including 30 samples was prepared from the above stock solutions. Correlation between concentrations of the desired cations was avoided. Appropriate amounts of  $\text{Zn}^{2+}$ ,  $\text{Cu}^{2+}$ , and  $\text{Cd}^{2+}$  solutions were transferred to 10 mL volumetric flasks, followed by the addition

of 2 mL of buffer solution and 0.6 mL of  $0.824 \text{ mmol L}^{-1}$  DMSPT. The solution then diluted to the mark with double-distilled water. The absorbance of each solution contains in 1 cm cell was measured with respect to a blank (double-distilled water).

**Preparation of Vegetable Samples.** Lettuce, dill, and tomato samples available on the local markets in Bushehr were purchased for investigation. First, samples were cleaned with tap water and double-distilled water. Then, the samples were dried at  $110 \text{ }^\circ\text{C}$ . Each of the dried varieties of samples was ground to reduce particle size and then thoroughly mixed to ensure homogeneity of samples individually. Masses of 500 mg were transferred into separate 250 mL beakers, and 5 mL of  $0.5 \text{ mol L}^{-1}$  nitric acid was added to moisten the samples thoroughly. This was followed by adding 10 mL of concentrated nitric acid and heating on a hot plate ( $130 \text{ }^\circ\text{C}$ ) for 3 h. After cooling to room temperature, 5 mL of concentrated perchloric acid was added dropwise. The beaker was heated gently until completion of sample decomposition, resulting in a clear solution. This was left to cool and then was transferred into a 100 mL volumetric flask by rinsing the interior of the beaker with small portions of  $0.1 \text{ mol L}^{-1}$  nitric acid, and the beaker was filled to the mark with the same acid.<sup>38</sup>

**Preparation of Rice Samples.** Ground rice (1.0 g) was digested with 10 mL of concentrated  $\text{HNO}_3$  at  $95 \text{ }^\circ\text{C}$ . The mixture was evaporated almost to dryness and mixed with 3 mL of  $\text{H}_2\text{O}_2$ . Then it was again evaporated to dryness. After evaporation, 8–9 mL of distilled water was added and the sample was mixed. The resulting mixture was filtered through a blue band filter paper. The filtrate was diluted to 100 mL with double-distilled water.<sup>40</sup>

## RESULTS AND DISCUSSION

**Preliminary Investigations.** Figure 1 shows the spectral data for  $\text{Zn}^{2+}$ ,  $\text{Cu}^{2+}$ , and  $\text{Cd}^{2+}$  complexes at optimum conditions

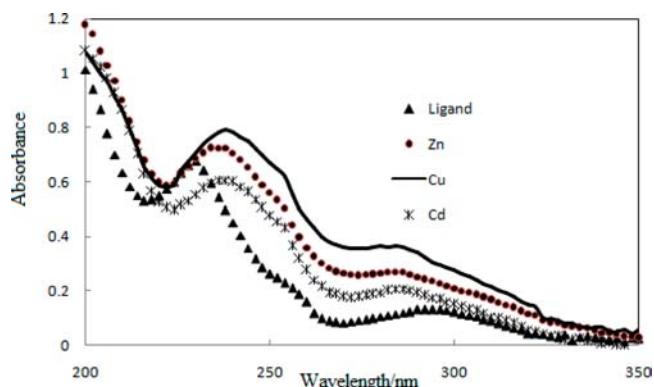


**Figure 1.** Absorption spectra for the solution of  $\text{Zn}^{2+}$  ( $2 \text{ mg L}^{-1}$ ),  $\text{Cu}^{2+}$  ( $1.5 \text{ mg mg L}^{-1}$ ), and  $\text{Cd}^{2+}$  ( $2 \text{ mg L}^{-1}$ ) in the presence of  $4.17 \times 10^{-5} \text{ mol L}^{-1}$  DMSPT at pH 6.7.

of pH 6.7 in the wavelength range of 200–350 nm. The composition of complexes was determined by a continuous variation method. A Job's plot for  $\text{Zn}^{2+}$ ,  $\text{Cu}^{2+}$ , and  $\text{Cd}^{2+}$  complexes confirmed a 1:1 (M:L) composition for all of the investigated complexes. Figure 1 illustrates the significant spectral overlap in the system at the considered conditions. Therefore, the metal ions interfere in the spectrophotometric determination of each other based on their complexation with DMSPT. Fortunately, combination of WT-FFNN can be a suitable method for the simultaneous determination of  $\text{Zn}^{2+}$ ,  $\text{Cu}^{2+}$ , and  $\text{Cd}^{2+}$  mixtures.

**Optimization of Experimental Conditions.** *Effect of pH.* The complex formation reactions of metal ions with DMSPT depend on pH. To find the optimum pH, the effect of pH in the range of 3.5–10.5 on the complex formation reactions of a constant concentration of each cation with DMSPT was



investigated (Figure 2). pH studies are carried out using sodium acetate–acetic acid (pH 3.5–5.0) and phosphate buffers (pH

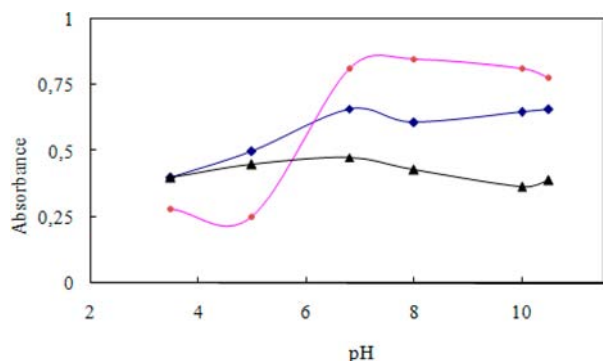


**Figure 2.** Effect of pH on absorbance signals of Zn<sup>2+</sup> (▲), Cu<sup>2+</sup> (□), and Cd<sup>2+</sup> (○).

6.0–10.5). From the results, it is observed that the complex exhibits maximum absorbance in the pH range of 6.0–8.0. Hence, further studies were carried out at pH 6.7 from phosphate buffer solution.

**Effect of Reagent Concentration.** The effect of DMSPT concentration over the range from 0.03 to 0.07 mmol L<sup>-1</sup> on the determination of 2.0 mg L<sup>-1</sup> each of Zn<sup>2+</sup>, Cu<sup>2+</sup>, Co<sup>2+</sup>, and Ni<sup>2+</sup> in pH 6.7 buffer solution was studied to obtain maximum color formation (Figure 3). Therefore, from the absorbance values, it is observed that 0.05 mmol L<sup>-1</sup> DMSPT is sufficient to get maximum complex formation.

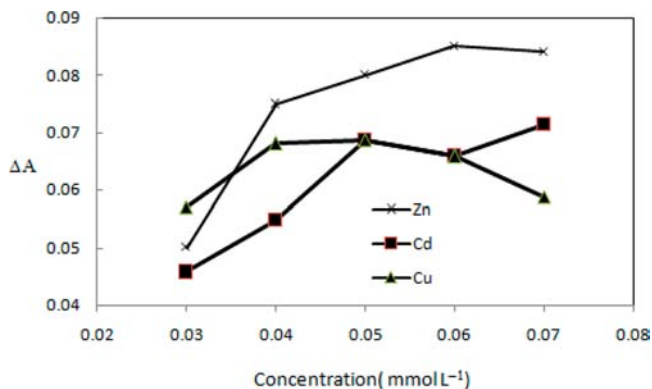


**Figure 3.** Effect of DMSPT concentration on ΔA signals of Zn<sup>2+</sup> (▲), Cu<sup>2+</sup> (□), and Cd<sup>2+</sup> (■).

**(a) Individual Calibration Graphs.** A set of sample solutions with different metal ion concentrations was prepared, and measurements were carried out under optimum conditions, according to the experimental procedure described under Optimization of Experimental Conditions. The calibration curves of analytes measured at different ranges were linear in the ranges of 0.6–7.0, 0.8–3.0, and 0.6–3.5 mmol L<sup>-1</sup> for Zn<sup>2+</sup>, Cd<sup>2+</sup>, and Cu<sup>2+</sup>, respectively. Typical equations of the calibration curves were as follows:  $A = 3.26 \times 10^{-1}C + 8.1 \times 10^{-2}$ ,  $r^2 = 0.996$ ;  $A = 8.81 \times 10^{-1}C + 1.7 \times 10^{-2}$ ,  $r^2 = 0.997$ ; and  $A = 3.06 \times 10^{-1}C + 2.5 \times 10^{-2}$ ,  $r^2 = 0.997$  for Zn<sup>2+</sup>, Cd<sup>2+</sup>, and Cu<sup>2+</sup>, respectively. Limit of detection (LODs) were determined as 0.046, 0.006, and 0.016 mmol L<sup>-1</sup> for Zn<sup>2+</sup>, Cd<sup>2+</sup>, and Cu<sup>2+</sup>, respectively. Also, limits of quantitations

(LOQs) were determined as 0.15, 0.060, and 0.16 mmol L<sup>-1</sup> for Zn<sup>2+</sup>, Cd<sup>2+</sup>, and Cu<sup>2+</sup>, respectively.

**(b) Detection of Nonlinearities.** Application of ANNs in multivariate calibrations was proposed when a significant nonlinearity was observed in the data.<sup>40</sup> A classical method to diagnose nonlinearity in multivariate calibration is to plot  $y$  versus each PC (partial response plot, PRP) or to plot the residuals ( $e_{PC_1-PCA}$ ) of the regression  $y = f(PC_1, \dots, PCA)$ , as

$$y = b_0 + b_1PC_1 + \dots + b_A PCA + b_a PCA + ey, PC_1-PCA \quad (4)$$

$$a = 1, \dots, A$$

against the fitted (predicted) response  $\hat{y}$  (residual plot, RP). A of eq 4 is the total number of PCs used.<sup>39</sup>

The relevant PRP plot was obtained by plotting the concentration as a function of PC1. Figure 4 shows the PRPs for the calibration of the three analytes, using PC1 for Cu<sup>2+</sup>, Cd<sup>2+</sup>, and Zn<sup>2+</sup>. PRP for the PC1 included in the model shows a nonlinear pattern. It is concluded that all investigated plots are able to detect strong nonlinearities presented in the system.

**(c) Reducing the Number of Data.** Decreasing the data volume before using ANNs for nonlinear multivariate calibration was suggested as a preprocessing step in many previous studies.<sup>31,37</sup> The most popular method for data compression in chemometrics is principal component analysis (PCA). Recently, we simply applied variance vector of WT as data compressing prior to ANN construction, for the determination of the enantiomeric composition of  $\alpha$ -phenylglycine.<sup>31</sup>

In this study, the applicability of WT for the simultaneous determination of ternary mixtures was examined, too. Wavelet coefficients belonging to maximum variances were used as indicators to select only small wavelength points from the whole spectral region, without loss of information. First, the wavelet transform was used to synthesize loadings for subjection to ANNs. Then the proposed procedure based on eq 3 was used for short data load to ANNs. Finally, the neural network was used to predict the approximation of the load for the simultaneous determinations.

**(d) Selection of Mother Wavelet and Level of Decomposition.** The mother wavelet and decomposition level, the best compression and smoothing of complex spectra, were chosen by taking into account the degree of similarity between the original data and the one reconstructed from approximation coefficients after compression. In this paper, the appropriate wavelets chosen from many types of the wavelets are meyr (meyr), morlet (morl), and symlet8 (sym8). WT was carried out in the optimum dilations: 15, 15, and 20 for meyr, morl, and sym8, respectively. Figure 5 shows the wavelet coefficients for selected mother wavelets for calibration set at optimum dilation values. Compression is achieved by eliminating the wavelet coefficients that do not hold valuable information. We are interested in keeping the systematic information in the data intact, and therefore the variance vector of the data set is a reasonable answer to which coefficients should be chosen.<sup>34</sup> Therefore, the variance vector was calculated by using eq 3. By extracting the positions of the variances between 70 and 95% values, wavelet coefficients were estimated. The selected wavelet coefficients of the optimal decomposition level are then used as input variable for ANN models. For each combination of parameters (wavelet filter, transforming, sorting, and selection criteria) the best performing ANN models corresponding to low RMSEP% and to a small number

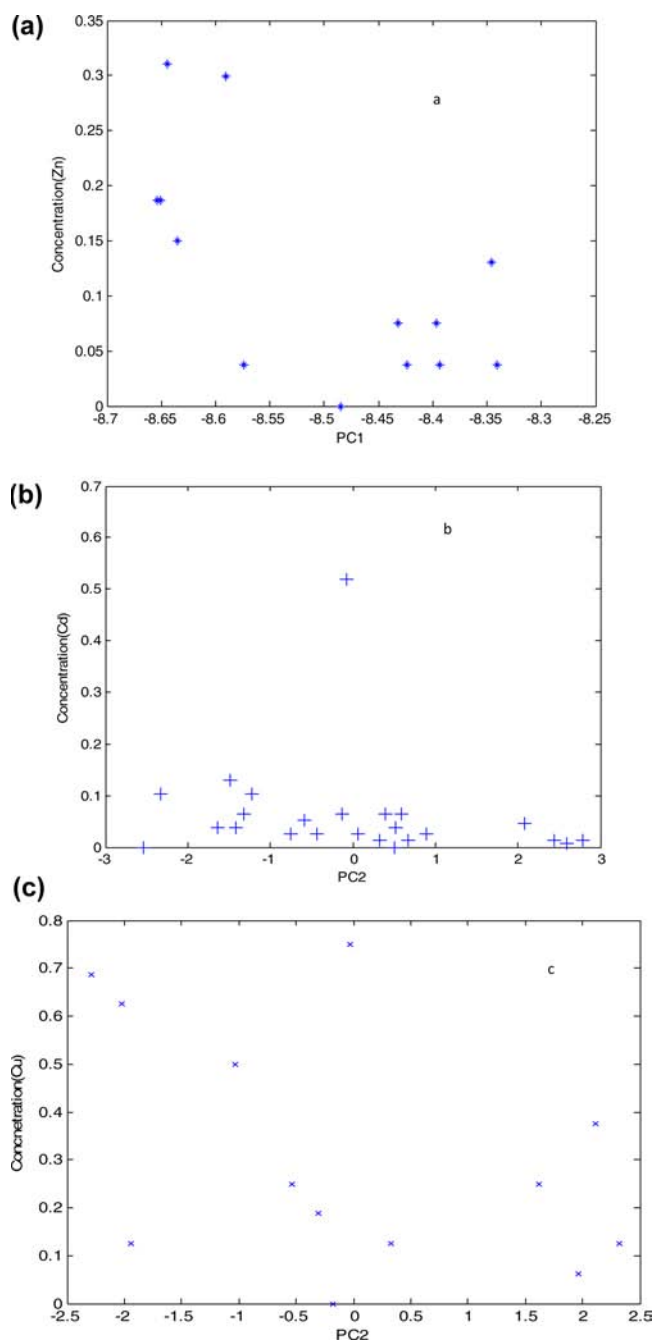


**Figure 4.** PRP plots for Cu (a), Zn (b), and Cd (c) considering PC1 and PC2 for nonlinearly detection.

of coefficients were selected. The numbers of selected wavelet coefficients were 80, 80, and 70 for morl, meyr, and sym8, respectively.

(e) *Construction of the WT-FFN Network.* To optimize the WT-FFNN architecture, the number of hidden layers was varied from one to five for metal ions. The root-mean-square errors prediction (RMSEP) for the prediction of analyte concentration was estimated. Criterion for illustration of the performance of the trained network is

$$\text{RMSEP} = \sqrt{\frac{\sum_{i=1}^n (\hat{y}_i - y_i)^2}{n}} \quad (5)$$

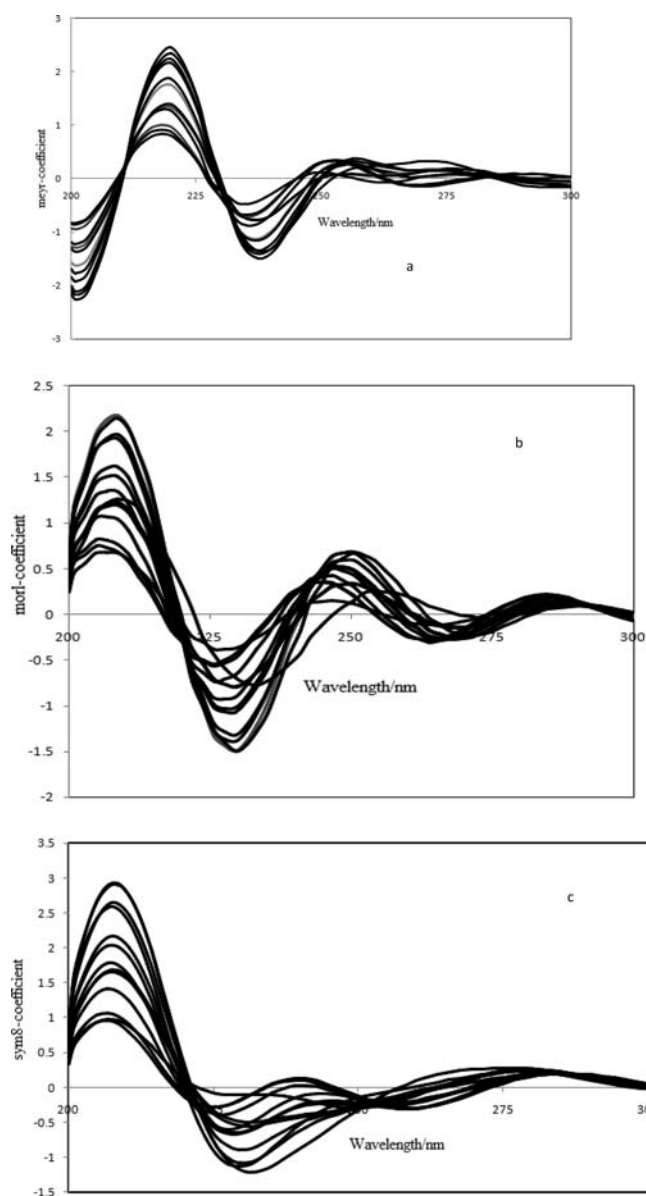


**Figure 5.** WT coefficient spectra on the calibration spectra using (a) meyr, (b) morl, and (c) sym8 at optimum dilation parameters.

where  $\hat{y}_i$  and  $y_i$  are the desired output and the actual output sets, respectively, and  $n$  is the number of prediction set samples. The validation set was applied to prevent the overfitting of the networks to the noise from the calibration set during training. The RMSE% values showed a minimum at one layer for all ions with morl and sym8 but two layers with meyr for  $\text{Zn}^{2+}$ . The number of input nodes (neurons) was selected as an optimal number of wavelet coefficients. To observe the extent of reproducibility of results and the robustness of the network, the training process in each condition was repeated five times. To determine the optimal number of hidden nodes, neural networks with different numbers of nodes were trained. Different transfer functions in hidden and output layers such as purelin, logsig, and tansig were also tested to obtain the best modeling network. For example, on the basis of data in Table 1, minimum RMSE% corresponds to position 3, which shows three nodes for hidden layers and learning functions logsig and logsig for hidden layer and output layer as optimums for

**Table 1. Optimized Parameters Used for Construction of WT-FFNN for Simultaneous Determination Zn<sup>2+</sup>, Cd<sup>2+</sup>, and Cu<sup>2+</sup> Using Different Mother Wavelets**

parameter	sym8			meyr			morl		
	Cu <sup>2+</sup>	Zn <sup>2+</sup>	Cd <sup>2+</sup>	Cu <sup>2+</sup>	Zn <sup>2+</sup>	Cd <sup>2+</sup>	Cu <sup>2+</sup>	Zn <sup>2+</sup>	Cd <sup>2+</sup>
hidden nodes	2	2	3	2	2	4	2	3	3
output nodes	1	1	1	1	1	1	1	1	1
epochs	200	200	200	180	180	180	200	200	200
hidden layer TF <sup>a</sup>	tansig	tansig	tansig	logsig	logsig	tansig	logsig	tansig	logsig
output layer TF <sup>a</sup>	tansig	tansig	tansig	tansig	tansig	tansig	tansig	tansig	logsig
learning rate	0.1	0.1	0.1	0.1	0.1	0.1	0.1	0.1	0.1

<sup>a</sup>Transfer function.

cadmium, respectively. The output layer was considered as a single node corresponding to an individual ion.

The best transfer functions as well as some other parameters such as number of epochs, learning rate, and momentum for Cu<sup>2+</sup>, Cd<sup>2+</sup>, and Zn<sup>2+</sup> with different mother wavelets are summarized in Table 1. Training the network was performed with several learning rates, which were changed from 0.01 to 0.1.

The predicted concentrations of three ions using the final obtained WT-FFNN models for prediction of set samples are given in Tables 2 and 3. The reasonable relative errors for each analyte indicate the accuracy of the proposed method.

**Table 2. Results for Metal Ions Analysis in Synthetic Samples by WT-FFNN Using meyr as Mother Wavelet**

actual concn (mmol L <sup>-1</sup> )			calcd concn (mmol L <sup>-1</sup> )		
Cd <sup>2+</sup>	Cu <sup>2+</sup>	Zn <sup>2+</sup>	Cd <sup>2+</sup>	Cu <sup>2+</sup>	Zn <sup>2+</sup>
0.030	0.250	0.037	0.030	0.251	0.037
0.012	0.625	0.187	0.011	0.622	0.188
0.064	0.375	0.14	0.064	0.377	0.151
0.052	0.625	0.038	0.054	0.624	0.038
0.038	1.00	0.187	0.038	1.000	0.188
0.518	0.50	0.150	0.518	0.500	0.151
0.103	0.750	0.30	0.104	0.756	0.311
0.026	0.625	0.15	0.025	0.625	0.150
0.104	0.812	0.04	0.105	0.812	0.038
0.064	0.00	0.074	0.064	0.000	0.074
0.00	0.50	0.224	0.000	0.500	0.000
%RMSEP			4.56	5.63	4.38

**Table 3. %RMSEP Values for Prediction Samples for Determination of Zn<sup>2+</sup>, Cd<sup>2+</sup>, and Cu<sup>2+</sup>**

mother wavelet	RMSEP, %		
	Zn <sup>2+</sup>	Cd <sup>2+</sup>	Cu <sup>2+</sup>
sym8	2.80	3.47	2.23
morl	2.57	1.53	2.40

(f) *Study of Interferences.* The interference study was performed by analyzing solutions containing 1.0 mg L<sup>-1</sup> Zn<sup>2+</sup>, Cd<sup>2+</sup>, and Cu<sup>2+</sup> ions in the presence of different ions. The tolerance limit was taken as the amount of added ions causing <5% relative error in the determination of Zn<sup>2+</sup>, Cd<sup>2+</sup>, and Cu<sup>2+</sup>. Table 4 summarizes the maximum tolerances of cations and anions. The results show that some metal ions at the levels given in Table 4 do not interfere under the experimental

**Table 4. Effect of Foreign Ions on the Simultaneous Determination Zn<sup>2+</sup>, Cd<sup>2+</sup>, and Cu<sup>2+</sup> (1.0 mg L<sup>-1</sup> of Each Metal Ion)**

foreign ion	tolerance limit (mg L <sup>-1</sup> )
Na <sup>+</sup> , K <sup>+</sup>	1000
F <sup>-</sup> , SO <sub>4</sub> <sup>2-</sup> , SCN <sup>-</sup>	>200
C <sub>2</sub> O <sub>4</sub> <sup>2-</sup>	>500
CH <sub>3</sub> CO <sub>2</sub> <sup>-</sup> , NO <sub>3</sub> <sup>-</sup>	30
Mn <sup>2+</sup>	500
Ag <sup>+</sup>	10
Fe <sup>3+</sup> , Ni <sup>2+</sup>	40
Hg <sup>2+</sup> , Pb <sup>2+</sup> , Cr <sup>3+</sup>	

conditions. We concluded that selectivity of newly synthetic ligand is very good.

**Applications.** Results for the analysis of synthetic mixtures by the proposed methods (Table 2) showed satisfactory results for the simultaneous determination of Zn<sup>2+</sup>, Cd<sup>2+</sup>, and Cu<sup>2+</sup>. To demonstrate the applicability of the optimized methods to real samples, it was applied to the simultaneous determination of Zn<sup>2+</sup>, Cd<sup>2+</sup>, and Cu<sup>2+</sup> in rice, tomato, dill, and lettuce samples containing desired elements at different levels. The results are shown in Table 5.

A comparison of the proposed method with the previously reported methods for determination of Cu<sup>2+</sup>, Zn<sup>2+</sup>, and Cd<sup>2+</sup> (Table 6) indicates that the proposed method is simpler than the existing methods and lower RSD% and better regression coefficients with respect to PLS and PCR. With respect to derivative methods provides better recoveries.

Comparison of our results with FAAS shows that the linear dynamic of the proposed method is wider than those obtained by FAAS (1–8, 0.5–1.5, and 0.5–3 mg L<sup>-1</sup> for Cu<sup>2+</sup>, Zn<sup>2+</sup>, and Cd<sup>2+</sup>, respectively). Atomic absorption spectrophotometry is not an absolute method of analysis, which can be a disadvantage when one is trying to analyze a mixture. Each element has to be tested separately. The samples and standards have to be in solution, or at least volatile. A large number of interferences are possible, such as the formation of nonvolatile compounds and smoke formation, which will absorb light, contamination, etc. Diverse ion investigation showed that synthetic ligand was very selective for the simultaneous determination of Cu<sup>2+</sup>, Zn<sup>2+</sup>, and Cd<sup>2+</sup> ions. With respect to our previous work, the tolerance limit of interfering ions (Hg<sup>2+</sup>, Pb<sup>2+</sup>, Ag<sup>+</sup>, and Mn<sup>2+</sup>) at the proposed method are larger than previous works.<sup>26</sup>

The results of synthetic and real mixtures show that a developed WT-FFNN method for the simultaneous determination of Zn<sup>2+</sup>, Cd<sup>2+</sup>, and Cu<sup>2+</sup> by the formation of yellow DMSPT complexes is very sensitive and much more

Table 5. Determination of Analyte Ions from Some Real Samples by WT-FFNN Using meyr, morl, and sym8 Mother Wavelets

sample	analyte	meyr			morl			sym8		
		added	found	recovery%	added	found	recovery%	added	found	recovery%
dill	Zn <sup>2+</sup>	0	0.85		0	0.62		0	0.66	
		2	2.87	101	2	2.64	106.6	2	2.68	101
	Cd <sup>2+</sup>	0	ND		0	ND		0	ND	
		2	2.05	102.5	2	2.1	105	2	2.01	100.5
	Cu <sup>2+</sup>	0	0.6		0	0.62		0	0.6	
		2	2.68	104	2	2.65	104.8	2	2.68	104
rice	Zn <sup>2+</sup>	0	2		0	2		0	2.0	
		2	3.98	99	2	4.03	101.5	2	4.05	102.5
	Cd <sup>2+</sup>	0	ND		0	ND		0	ND	
		2	2.01	101	2	2.01	100.5	2	2.1	105
	Cu <sup>2+</sup>	0	0.5		0	0.55		0	0.51	
		2	2.51	100.5	2	2.58	105.4	2	2.53	101
tomato	Zn <sup>2+</sup>	0	0.6		0	0.62		0	0.6	
		2	2.64	102	2	2.65	104.8	2	2.65	102.5
	Cd <sup>2+</sup>	0	0.02		0	0.023		0	0.02	
		2	2.03	100.5	2	2.03	100.4	2	2.03	100.5
	Cu <sup>2+</sup>	0	0.3		0	0.4		0	0.38	
		2	2.32	101	2	2.42	101	2	2.40	101
lettuce	Zn <sup>2+</sup>	0	0.52		0	0.50		0	0.54	
		2	2.48	98	2	2.48	99	2	2.56	101
	Cd <sup>2+</sup>	0	ND		0	ND		0	ND	
		2	1.96	98	2	2.01	100.5	2	2.03	101.5
	Cu <sup>2+</sup>	0	0.53		0	0.54		0	0.54	
		2	2.55	103.8	2	2.56	101	2	2.56	101

Table 6. Comparison of the Performance of the Proposed Method with Reported Methods

method	ion	linearity	LOD	RSD%	r <sup>2</sup>	calibration equation	ref
derivative potentiometry	Zn <sup>2+</sup>					$A = 3.9 \times 10^7 C + 2.7 \times 10^5$	11
	Cd <sup>2+</sup>					$A = 5.3 \times 10^7 C + 2.6 \times 10^5$	
FAAS	Zn <sup>2+</sup>		0.12 <sup>a</sup>	5–9		$A = 0.391C + 0.006$	4
	Cu <sup>2+</sup>		0.12 <sup>a</sup>	5–8		$A = 0.111C + 0.008$	
PLS	Zn <sup>2+</sup>	0–0.7		8.79	0.9926	$A = 1.3108C + 0.304$	24
	Cd <sup>2+</sup>	0–3.96		5.22	0.9950	$A = 0.0192C + 0.3291$	
PCR	Zn <sup>2+</sup>	0–0.7		9.93	0.889	$A = 1.3108C + 0.304$	
	Cd <sup>2+</sup>	0–3.96		17.68	0.636	$A = 0.0192C + 0.3291$	
FAAS-cloud point extraction	Zn <sup>2+</sup>	0.095–50	0.095 <sup>b</sup>	1.5	0.999	$A = 0.0019C + 0.029$	6
	Cd <sup>2+</sup>	0.099–50	0.099 <sup>b</sup>	3.1	0.9982	$A = 0.0012C + 0.014$	
	Cu <sup>2+</sup>	0.27–100	0.27 <sup>b</sup>	1.6	0.9987	$A = 0.045C + 0.014$	
ANNs	Zn <sup>2+</sup>	0.5–12	0.056		0.9979	$A = 7.88 \times 10^{-2} C + 2.3 \times 10^{-3}$	25
	Cu <sup>2+</sup>	1.0–12	0.108		0.9989	$A = 1.81 \times 10^{-1} C + 2.0 \times 10^{-2}$	
ICP-OES	Cu <sup>2+</sup>		0.23	3.38		$A = 4.20C + 7.57$	8
	Cd <sup>2+</sup>		0.02	5.06		$A = 22.79C + 221.69$	

<sup>a</sup>mg kg<sup>-1</sup>. <sup>b</sup>ng mL<sup>-1</sup>.

quantitative rather than earlier methods (PCA-ANNs).<sup>24</sup> The results obtained with selection of wavelet coefficient gives generally lower RMSEP% (for Zn<sup>2+</sup> and Cu<sup>2+</sup> between 1.53 and 2.80) with respect to the PCA selection criteria of our previous work (for Zn<sup>2+</sup> and Cu<sup>2+</sup> between 1.24 and 4.81). It can be seen

that the variance sorting criterion performs generally better with respect to the other regression one, giving on average lower values of RMSEP%.

In this work we have shown that WT can be effectively coupled to predictive feature selection criteria, by containing



maximum variance, to find the minimum number of best performing wavelet coefficients. These coefficients constitute a new set of predictor variables that can be passed to ANN models. The short loaded significant wavelength coefficients decrease the contribution of experimental noise and other minor factors. The method does not decrease the S/N ratio, and so it can be used for routine analysis of  $Zn^{2+}$ ,  $Cd^{2+}$ , and  $Cu^{2+}$  in different mixtures. The proposed procedures allowed us the simultaneous determination of  $Zn^{2+}$ ,  $Cd^{2+}$ , and  $Cu^{2+}$  ions, for which absorption spectra were seriously overlapped under the experimental conditions. Hence, the results showed that the key concepts of the proposed procedure overcome the main drawback related to the heavily overlapped spectra of the component of a solution. Even the presence of high spectral overlapping limits the use of these methods, but the localized nature of the wavelet transformation overcomes the problem due to the strong overlapping of spectra. In conclusion, the method proposed in this work provides a time-saving procedure without any separation steps and good results with low prediction errors for the simultaneous determination of  $Zn^{2+}$ ,  $Cd^{2+}$ , and  $Cu^{2+}$  ions.

## AUTHOR INFORMATION

### Funding

We thank the Persian Gulf University research council for their support under Grant PGU/FS/45-2/1391/1956.

### Notes

The authors declare no competing financial interest.

## REFERENCES

- (1) Golhaber, S. B. Trace element risk assessment: essentially vs. toxicity. *Regul. Toxicol. Pharmacol.* **2003**, *38*, 232–242.
- (2) Igoe, S. R.; Hui, Y. H. *Dictionary of Food Ingredients*, 4th ed.; Aspen Publishers: Gaithersburg, MD, 2001.
- (3) Balch, A. *Prescription for Nutritional Healing: an easy to A-Z references to Hundreds of Common Disorders and Their Herbal Remedies*; Penguin Press: New York, 2006; pp 431, 534.
- (4) Nunes, L. S.; Barbosa, J. T. P.; Fernandes, A. P.; Lemos, V. A.; Santos, W. N. L.; Korn, M. G. A.; Teixeira, L. S.G. Multi-element determination of Cu, Fe, Ni and Zn content in vegetable oils samples by high-resolution continuum source atomic absorption spectrometry and microemulsion sample preparation. *Food Chem.* **2011**, *127*, 780–783.
- (5) Mondal, B. C.; Das, D.; Das, A. K. Preconcentration and separation of copper, zinc and cadmium by the use of 6-mercaptopyridinylazo resin and their application in microwave digested certified biological samples followed by AAS determination of the metal ions. *J. Trace Elem. Med. Biol.* **2002**, *16*, 145–148.
- (6) Chen, J.; Teo, K. C. Determination of cadmium, copper, lead and zinc in water samples by flame atomic absorption spectrometry after cloud point extraction. *Anal. Chim. Acta* **2001**, *450*, 215–222.
- (7) dos Santos, L. M. G.; Welz, B.; Araujo, R. G. O.; Jacob, S. do C.; Vale, S.; Martens, M. G. R.; Martens, A.; Becker-Ross, I. B. G. H. Simultaneous determination of Cd and Fe in beans and soil of different regions of Brazil using high-resolution continuum source graphite furnace atomic absorption spectrometry and direct solid sampling. *J. Agric. Food Chem.* **2009**, *57*, 10089–10094.
- (8) Bezerra, M. A.; dos Santos, W. N. L.; Lemos, V. A.; Korn, M. G. A.; Ferreria, S. L. C. On line system for preconcentration and determination of metals in vegetables by inductively coupled plasma optical emission spectrometry. *J. Hazard. Mater.* **2007**, *148*, 334–339.
- (9) Rodriguez, A. M. G.; Torres, A. G.; Pavon, J. M. C.; Ojeda, C. B. Simultaneous spectrophotometric determination of cadmium, copper and zinc. *Talanta* **1993**, *40*, 1861–1866.
- (10) Beinrohr, E.; Tschöpel, P.; Tölg, G.; Németh, M. Flow-through anodic stripping coulometry and anodic stripping coulometry with collection for the simultaneous absolute determination of copper, lead, cadmium and zinc. *Anal. Chim. Acta* **1993**, *273*, 13–25.
- (11) Lo Coco, F.; Cecon, L.; Ciraolo, L.; Novelli, V. Determination of cadmium(II) and zinc(II) in olive oils by derivative potentiometric stripping analysis. *Food Control* **2003**, *14*, 55–59.
- (12) La Pera, L.; Saitta, M.; Bella, G. D.; Dugo, G. Simultaneous determination of Cd(II), Cu(II), Pb(II), and Zn(II) in citrus essential oils by derivative potentiometric stripping analysis. *J. Agric. Food Chem.* **2003**, *51*, 1125–1129.
- (13) Themelis, D. G.; Paraskevas, D. T.; Anastasios, V. T.; Sofoniou, C. M. Direct and selective flow-injection method for the simultaneous spectrophotometric determination of calcium and magnesium in red and white wines using online dilution based on “zone sampling”. *J. Agric. Food Chem.* **2001**, *49*, 5152–5155.
- (14) Mashhadizadeh, M. H.; Karami, Z. Solid phase extraction of trace amounts of Ag, Cd, Cu, and Zn in environmental samples using magnetic nanoparticles coated by 3-(trimethoxysilyl)-1-propanol and modified with 2-amino-5-mercapto-1,3,4-thiadiazole and their determination by ICP-OES. *J. Hazard. Mater.* **2011**, *190*, 1023–1029.
- (15) Fredrikson, M.; Carlsson, N. G.; Almgren, A.; Sandberg, A. S. Simultaneous and sensitive analysis of Cu, Ni, Zn, Co, Mn, and Fe in food and biological samples by ion chromatography. *J. Agric. Food Chem.* **2002**, *50*, 59–65.
- (16) Narin, I.; Soylak, M. Enrichment and determinations of nickel(II), cadmium(II), copper(II), cobalt(II) and lead(II) ions in natural waters, table salts, tea and urine samples as pyrrolydine dithiocarbamate chelates by membrane filtration–flame atomic absorption spectrometry combination. *Anal. Chim. Acta* **2003**, *493*, 205–212.
- (17) Soylak, M.; Tuzen, M.; Souza, S. A.; das Gracias Andrade Korn, M.; Costa Ferreira, S. L. Optimization of microwave assisted digestion procedure for the determination of zinc, copper and nickel in tea samples employing flame atomic absorption spectrometry. *J. Hazard. Mater.* **2007**, *149*, 264–268.
- (18) Tuzen, M.; Silici, S.; Mendil, D.; Soylak, M. Trace element levels in honeys from different regions of Turkey. *Food Chem.* **2007**, *103*, 325–330.
- (19) Pohl, P.; Prusisz, B. Determination of Ca, Mg, Fe and Zn partitioning in UHT cow milks by two-column ion exchange and flame atomic absorption spectrometry detection. *Talanta* **2007**, *71*, 715–721.
- (20) [http://vedyadhara.ignou.ac.in/wiki/images/d/d8/Unit\\_9\\_Atomic\\_Absorption](http://vedyadhara.ignou.ac.in/wiki/images/d/d8/Unit_9_Atomic_Absorption).
- (21) Ghaedi, M. Pyrimidine-2-thiol as selective and sensitive ligand for preconcentration and determination of  $Pb^{2+}$ . *Chem. Anal.* **2006**, *51*, 593–602.
- (22) Pehlivan, E.; Gode, F. Batch sorption of divalent metal ions onto brown coal. *Energy Sources Part A* **2006**, *28*, 1493–1508.
- (23) Shampur, T.; Mashhadizadeh, M. H.; Sheikhshoae, I. Flame atomic absorption spectrometric determination of silver ion after preconcentration on octadecyl silica membrane disk modified with bis[5-((4-nitrophenyl)azosalicylaldehyde)] as a new Schiff base ligand. *J. Anal. At. Spectrosc.* **2003**, *18*, 1407–1410.
- (24) Gao, L.; Ren, S. Simultaneous spectrophotometric determination of four metals by two kinds of partial least squares methods. *Spectrochim. Acta A* **2005**, *61*, 3013–3019.
- (25) Rouhollahi, A.; Tavakoli, H.; Nayeibi, S. Simultaneous spectrophotometric determination of heavy metal ions using several chemometrics methods: effect of different parameters of Savitzky-Golay and direct orthogonal signal correction filters. *Iran J. Chem. Chem. Eng.* **2007**, *26*, 41–51.
- (26) Afkhami, A.; Abbasi-Tarighat, M.; Khanmohammadi, H. Simultaneous determination of  $Co^{2+}$ ,  $Ni^{2+}$ ,  $Cu^{2+}$  and  $Zn^{2+}$  ions in foodstuffs and vegetables with a new Schiff base using artificial neural networks. *Talanta* **2009**, *77*, 995–1001.
- (27) Ensafi, A. A.; Khayamian, T.; Benvidi, A.; Mirmomtaz, E. simultaneous determination of copper, lead and cadmium by cathodic adsorptive stripping voltammetry using artificial neural networks. *Anal. Chim. Acta* **2006**, *561*, 225–232.



(28) Cocchi, M.; Hidalgo-Hidalgo-de-Cisneros, J. L.; Naranjo-Rodriguez, I.; Palacios Santander, J. M.; Seeber, R.; Ulrici, A. Multicomponent analysis of electrochemical signal in the wavelet domain. *Talanta* **2003**, *59*, 735–749.

(29) Dinç, E.; Baleanu, D. A zero-crossing technique for the multidetermination of thiamine HCl and pyridoxine HCl in their mixture by using one-dimensional wavelet transform. *J. Pharm. Biomed. Anal.* **2003**, *31*, 969–978.

(30) Dinç, E.; Baleanu, D. Multicomponent quantitative resolution of binary mixtures by using continuous wavelet transform. *J. AOAC Int.* **2004**, *87*, 360–365.

(31) Afkhami, A.; Abbasi-Tarighat, M.; Bahram, M. Artificial neural networks for determination of enantiomeric composition of  $\alpha$ -phenylglycine using UV spectra of cyclodextrin host guest complexes. Comparison of feed-forward and radial basis function networks. *Talanta* **2008**, *75*, 91–96.

(32) Afkhami, A.; Madrakian, T.; Abbasi-Tarighat, M. Simultaneous determination of calcium, magnesium and zinc in different foodstuffs and pharmaceutical samples with continuous wavelet transforms. *Food Chem.* **2008**, *109*, 660–669.

(33) Abbasi Tarighat, M. Kinetic-spectrophotometric determination of tin species using feed-forward neural network and radial basis function networks in water and juices of canned fruit. *Anal. Chem. Indian J.* **2013**, *12*, 256–263.

(34) Abbasi Tarighat, M.; Shahbazi, E.; Niknam, Kh. Simultaneous determination of  $Mn^{2+}$  and  $Fe^{3+}$  as 4,4'-[(4-chlorophenyl)methylene] bis(3-methyl-1-phenyl-1H-pyrazol-5-ol) complexes in some foods, vegetable and water samples by artificial neural networks. *Food Chem.* **2013**, *138*, 991–997.

(35) Abbasi Tarighat, M.; Afkhami, A. Simultaneous spectrophotometric determination of Cu(II), Co(II) and Ni(II) using ratio spectra continuous wavelet transformation in some food and environmental samples. *J. Braz. Chem. Soc.* **2012**, *0*, 1–8.

(36) Mallat, S. *A Wavelet Tour of Signal Processing: The Sparse Way*, 3ed.; Academic Press: San Diego, CA, 2009.

(37) Cai, C. S.; Harrington, P. D. Different discrete wavelet transforms applied to denoising analytical data. *J. Chem. Inf. Comput. Sci.* **1998**, *38*, 1161–1170.

(38) Xiaoquan, L.; Hongde, L.; Zhonghua, X.; Qiang, Z. Maximum spectrum of continuous wavelet transform and its application in resolving an overlapped signal. *J. Chem. Inf. Comput. Sci.* **2004**, *44*, 1228–1237.

(39) Baytak, S. Solid-phase extractor with ram horn powder for lead and cadmium determination in environmental samples by flame atomic absorption spectrometry. *Acta Chim. Slov.* **2007**, *54*, 385–391.

(40) Centner, V.; de Noord, O. E.; Massart, D. L. Detection of nonlinearity in multivariate calibration. *Anal. Chim. Acta* **1998**, *376*, 153–158.